Optics Communications 285 (2012) 766–773

Contents lists available at SciVerse ScienceDirect

Optics Communications

journal homepage: www.elsevier.com/locate/optcom

Peculiarities of thermo-optic coefficient under different temperature regimes in optical fibers containing fiber Bragg gratings

Grigory Adamovsky [a], Sergei F. Lyuksyutov [d,*], Jeffrey R. Mackey [b], Bertram M. Floyd [c], Ujitha Abeywickrema [d], Igor Fedin [d], Mindaugas Rackaitis [e]

[a] NASA, John H. Glenn Research Center, Cleveland OH 44135, United States
[b] ASRC Aerospace Corporation, Cleveland OH 44135, United States
[c] Sierra Lobo, Inc., Cleveland OH 44135, United States
[d] Department of Physics, University of Akron, Akron OH 44325, United States
[e] Bridgestone Americas, Center for Research and Technology, Akron OH 44317, United States

ARTICLE INFO

Article history:
Received 20 May 2011
Received in revised form 25 July 2011
Accepted 31 October 2011
Available online 15 November 2011

Keywords:
Optical materials
Optical fibers
Bragg gratings
Thermodynamic properties
High temperature tests

ABSTRACT

Direct experimental measurements of the thermo-optic for fixed temperature intervals (20–200 °C, 200–500 °C, 500–660 °C, 660–780 °C) in fused silica fiber containing fiber Bragg gratings (FBGs) were conducted. The diffraction efficiency of a FBG fluctuated with temperature between 2.01×10^{-4} and 0.17×10^{-4} while the temperature shift of the Bragg's peak was monitored between 1300 and 1311 nm with sub-Angstrom precision. Numerical simulations were focused on FBG's diffraction efficiency calculations accounting for the temperature drift of the gratings, and found to be in excellent agreement with obtained experimental data.

It was found that the first-order thermo-optic coefficient changes between 1.29 and $1.85\times10^{-5}\,K^{-1}$ for the linear fit and at T = 0 °C its value was found to be close to $2.37\times10^{-5}\,K^{-1}$ for the polynomial fit of experimental data. The average thermo-optic coefficient undergoes a minimum in the vicinity of 440 °C. Additional observation indicates a negative sign of the second-order thermo-optic coefficient. The value of thermal expansion coefficient was much less ($0.5\times10^{-6}\,K^{-1}$) than that for the average thermo-optic coefficient. Based on the energy dispersive spectroscopy it was determined that thermal erasing of the FBGs at a temperature around 780 °C corresponds to germanium monoxide diffusion out of core in silica-based fibers.

1. Introduction

The temperature dependence of thermo-optic and thermal expansion coefficients in silica-based fibers containing fiber Bragg gratings (FBGs) [1,2] involves a wide range of thermal phenomena such as thermal stability of chemical composition gratings [3], non-linear temperature dependence of FBGs written in different fibers [4], quadratic behavior of FBGs [5], and long-term stability of silica-based FBGs [6].

Sensors based on FBGs have different applications and ability to accurately measure such physical parameters as temperature, strain, pressure, and acceleration while being relatively immune to the electromagnetic interference. Until recently the major obstacle in introducing FBG-based sensors into engine flight control was temperature limitation (1000 °C and above). It was reported [6–8] that the FBG-based sensors withstood temperatures at around 900 °C for relatively long periods of time. Very recently, pressure sensors based on mechanically-induced FBG [9], optical fiber tip sensors [10] and high-temperature multi-parameter sensors based on a sapphire FBG [11] have also been developed.

However, experimental studies of thermal expansion and thermo-optical effects in silica-based fibers reported so far have neither included theoretical versus experimental comparison of Bragg peak strength and shift with temperature nor the separation of the two effects one from another.

Our goal was to investigate both experimentally (with *IR* light) and theoretically a Bragg peak shift for four different temperature regimes, 50–200 °C, 200–500 °C, 500–660 °C, and 660–780 °C, in silica-based fibers containing FBG sensors. Based on this analysis, we assessed specifics of the thermal optical and thermal expansion coefficients' behavior.

2. Experimental setup

The experimental setup containing two light sources is shown in Fig. 1. One light source is a 20 mW laser operating at 550 nm wavelength and the other one is a superluminescent laser diode (SLD) emitting 5 mW of infrared radiation with the central wavelength of

* Corresponding author. Tel.: +330 972 8356.
E-mail address: sfl@uakron.edu (S.F. Lyuksyutov).

0030-4018/$ – see front matter © 2011 Elsevier B.V. All rights reserved.
doi:10.1016/j.optcom.2011.10.084

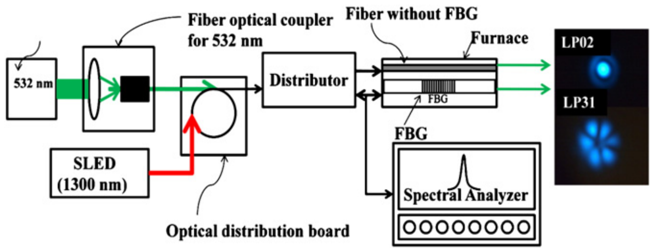

Fig. 1. Schematic presentation of experimental setup.

about 1310 nm and a minimum bandwidth about 20 nm. Light from both sources is coupled into two identical pieces of a commercial optical fiber with core diameter of about 9.15 μm using an optical distribution board. One of the fibers contains an optical Bragg grating (FBG) written into it. The peak wavelength of the FBG at 20 °C is about 1300.135 nm and bandwidth is between 16.8 and 25.7 GHz for 1 and 3 dB respectively. Both fibers are placed in ceramic capillary tubes and put inside a 24″ long 1200 °C split hinge tube furnace in such a way that the FBG is approximately in the middle of the furnace heating tube. The temperature of the tube furnace is controlled in the range 20–1200 °C.

A portion of the infrared radiation from the SLD is reflected from the FBG and is detected by a photodetector incorporated inside of an optical spectrum analyzer (OSA). As the temperature in the furnace changes, the wavelength of the radiation reflected by the FBG and detected by the OSA changes as well. Those changes are displayed on the screen of the OSA.

Radiation at the visible wavelength passes through both fibers and is then observed on a screen in the form of two patterns. One pattern is generated by a portion of that radiation passed through a fiber containing the FBG and the other one by radiation passed through the fiber without the FBG. The transmitted visible light is also collected, analyzed and recorded with a CCD camera to monitor distribution of the observed linearly polarized (LP) modes in the samples with and without the FBG.

Diffraction efficiency of the FBG was measured by calculating the power ratio of light reflected on the FBG (peak intensity as shown in Fig. 3) with respect to the coupled light (power varied between 1 and 3 mW).

The losses on couplers/splitters (insertion loss 3.13 dB), interconnectors (insertion loss 1 dB) and a circulator (insertion loss 0.43 dB) were taken into account for the wavelength range 1270–1350 nm.

3. Theoretical principles

Diffraction efficiency of a FBG embedded in optical fibers can be presented in a general case using the solution of coupled wave equations [12,13] as:

$$\eta = \frac{\sinh^2(\gamma\Lambda)}{\cosh^2(\gamma\Lambda) - \frac{\Delta}{k}} \tag{1}$$

where, $\gamma = \sqrt{k^2 - \Delta^2}$, and the parameters k and Δ can be written as:

$$k = \left(\frac{\pi}{\lambda}\right)x10^{-4} \text{ and } \Delta = \frac{2\pi n_{eff}}{\lambda} - \frac{\pi}{\Lambda(T)} = \frac{2\pi n_{eff}}{\lambda} - \frac{\pi}{\Lambda(1+\alpha_T T + \beta_T T^2 + \gamma T^3)}$$

In this study, the thermal optical and thermal expansion effects were introduced separately:

$$n_{\text{eff}} = n_0 + a\text{T} + \beta\text{T}^2 + \gamma\text{T}^3$$

for the thermal optical change of refractive index, and

$$\Lambda = \Lambda_0\left(1 + a_T T + \beta_T T^2 + \gamma_T T^3\right)$$

for the thermal expansion of the grating, where α,β, and γ are the thermo-optic coefficients of the first (α), second (β) and third (γ) orders respectively:

$$\alpha = \left(\frac{\partial n}{\partial T}\right)_{T=0}, \quad \beta = \frac{1}{2!}\left(\frac{\partial^2 n}{\partial T^2}\right)_{T=0}, \text{and} \quad \gamma = \frac{1}{3!}\left(\frac{\partial^3 n}{\partial T^3}\right)_{T=0};$$

with refractive index $n_0 = 1.4669$ calculated from data fitting parameters at $T = 0$ °C.

The thermal expansion coefficients of the first (α_T), second (β_T), and the third (γ_T) orders can be expressed as:

$$\alpha_t = \frac{1}{\Lambda_0}\left(\frac{\partial\Lambda}{\partial T}\right)_{T=0}, \beta_t = \frac{1}{2!}\frac{1}{\Lambda_0}\left(\partial^2\frac{\Lambda}{\partial T^2}\right)_{T=0}, \text{and} \quad \gamma_t = \frac{1}{3!}\frac{1}{\Lambda_0}\left(\frac{\partial^3\Lambda}{\partial T^3}\right)_{T=0}$$

The Bragg wavelength λ_B depends on the effective refractive index of the fiber n_{eff} and the grating period Λ as:

$$\lambda_B = 2n_{\text{eff}}\Lambda \tag{2}$$

The shift of λ_B in Eq. (2) with temperature occurs due to both, the temperature dependence of the refractive index n and the thermal expansion of the fiber [4]. Now we can express the Bragg wavelength for arbitrary temperature T in terms of λ_{B0} (also called the Bragg peak wavelength at $T_0 = 0$ °C):

$$\begin{aligned}\lambda_B &= 2n\Lambda = 2\cdot\left(n_0 + \alpha T + \beta T^2 + \gamma T^3 + \ldots\right)\cdot\Lambda_0\left(1 + \alpha_T T + \beta_T T^2 + \gamma_T T^3 + \ldots\right) = \\ &= 2n_0\Lambda_0\left(1 + \frac{\alpha}{n_0}T + \frac{\beta}{n_0}T^2 + \frac{\gamma}{n_0}T^3 + \ldots\right)\cdot\left(1 + \alpha_T T + \beta_T T^2 + \gamma_T T^3 + \ldots\right) = \\ &= \lambda_{B0}\cdot\left(1 + \left(\frac{\alpha}{n_0} + \alpha_T\right)\cdot T + \left(\frac{\beta}{n_0} + \beta_T + \frac{\alpha\alpha_T}{n_0}\right)\cdot T^2 \right. \\ &\quad \left. + \left(\frac{\gamma}{n_0} + \gamma_T + \frac{\alpha\beta_T}{n_0} + \frac{\beta\alpha_T}{n_0} + \right)\cdot T^3 + \ldots\right)\end{aligned} \tag{3}$$

Another representation of formula (3) is:

$$\begin{aligned}\lambda_B &= \lambda_{B0} + B_1 T + B_2 T^2 + B_3 T^3 + \ldots \\ &= \lambda_{B0}\left(1 + B_1{}'T + B_2{}'T^2 + B_3{}'T^3 + \ldots\right)\end{aligned} \tag{4}$$

Polynomial and linear fittings of experimental data are to be performed separately with the fitting parameters ($B_1{}'$,$B_2{}'$,$B_3{}'$) of interest below:

$$\begin{aligned}\frac{B_1}{\lambda_{B0}} &= B_1{}' = \frac{\alpha}{n_0} + \alpha_T \\ \frac{B_2}{\lambda_{B0}} &= B_2{}' = \frac{\beta}{n_0} + \beta_T + \frac{\alpha\alpha_T}{n_0} \\ \frac{B_3}{\lambda_{B0}} &= B_3{}' = \frac{\gamma}{n_0} + \gamma_T + \frac{\alpha\beta_T}{n_0} + \frac{\beta\alpha_T}{n_0}\end{aligned} \tag{5}$$

4. Results and discussion

4.1. Diffraction efficiency and shift of the Bragg peak

The diffraction efficiency of the FBGs in different samples was analyzed and found to be dependent strongly on a temperature change. In the range of temperatures between 20 and 660 °C the efficiency varied slightly from 1.63×10^{-4} to 2.01×10^{-4}, while between 670 and 780 °C the diffraction efficiency sharply declined from 1.92×10^{-4} down to 0.17×10^{-4} when the grating vanished at the temperature between 780 and 790 °C. Experimental dependence